Since January 2020 Elsevier has created a COVID-19 resource centre with free information in English and Mandarin on the novel coronavirus COVID-19. The COVID-19 resource centre is hosted on Elsevier Connect, the company's public news and information website.

Journal of Trace Elements in Medicine and Biology 68 (2021) 126818

Contents lists available at ScienceDirect

Journal of Trace Elements in Medicine and Biology

journal homepage: www.elsevier.com/locate/jtemb

Evaluation of *in vitro* activity of copper gluconate against SARS-CoV-2 using confocal microscopy-based high content screening

Killian Rodriguez [a,1], Florian Saunier [a,b,1], Josselin Rigaill [a,c], Estelle Audoux [a], Elisabeth Botelho-Nevers [a,b], Amélie Prier [a], Yann Dickerscheit [a], Sylvie Pillet [a,c], Bruno Pozzetto [a,c], Thomas Bourlet [a,c], Paul O. Verhoeven [a,c,*]

[a] CIRI, Centre International de Recherche en Infectiologie, GIMAP team, University of Lyon, University of St-Etienne, INSERM U1111, CNRS UMR5308, ENS de Lyon, UCBL1, St-Etienne, France
[b] Infectious Diseases Department, University Hospital of St-Etienne, France
[c] Department of Infectious Agents and Hygiene, University Hospital of St-Etienne, France

ARTICLE INFO

Keywords:
SARS-CoV-2
Copper gluconate
Vero E6 cells

ABSTRACT

Context: Severe Acute Respiratory Syndrome Coronavirus 2 (SARS-CoV-2) that emerged late in 2019 is the etiologic agent of coronavirus disease 2019 (Covid-19). There is an urgent need to develop curative and preventive therapeutics to limit the current pandemic and to prevent the re-emergence of Covid-19. This study aimed to assess the *in vitro* activity of copper gluconate against SARS-CoV-2.

Methods: Vero E6 cells were cultured with or without copper gluconate 18−24 hours before infection. Cells were infected with a recombinant GFP expressing SARS-CoV-2. Cells were infected with a recombinant GFP expressing SARS-CoV-2. Infected cells were incubated in fresh medium containing varying concentration of copper gluconate (supplemented with bovine serum albumin or not) for an additional 48 -h period. The infection level was measured by the confocal microscopy-based high content screening method. The cell viability in presence of copper gluconate was assessed by XTT and propidium iodide assays.

Results: The viability of Vero E6 cells exposed to copper gluconate up to 200 μM was found to be similar to that of unexposed cells, but it dropped below 70 % with 400 μM of this agent after 72 h of continuous exposure. The infection rate was 23.8 %, 18.9 %, 20.6 %, 6.9 %, 5.3 % and 5.2 % in cells treated prior infection with 0, 2, 10, 25, 50 and 100 μM of copper gluconate respectively. As compared to untreated cells, the number of infected cells was reduced by 71 %, 77 %, and 78 % with 25, 50, and 100 μM of copper gluconate respectively ($p < 0.05$). In cells treated only post-infection, the rate of infection dropped by 73 % with 100 μM of copper gluconate ($p < 0.05$). However, the antiviral activity of copper gluconate was abolished by the addition of bovine serum albumin.

Conclusion: Copper gluconate was found to mitigate SARS-CoV-2 infection in Vero E6 cells but this effect was abolished by albumin, which suggests that copper will not retain its activity in serum. Furthers studies are needed to investigate whether copper gluconate could be of benefit in mucosal administration such as mouthwash, nasal spray or aerosols.

1. Introduction

At the end of 2019, the emergence of a novel coronavirus designated as Severe Acute Respiratory Syndrome Coronavirus 2 (SARS-CoV-2) has led to a pandemic that threatens human health and public safety [1,2]. This new virus is highly transmissible and has spread very fast all over the world [1]. Even though the great majority of people (i.e. around 80 %) develop mild to moderate coronavirus disease 2019 (Covid-19), a significant proportion of cases are severe or critical and can lead to death [1,3]. So far 3,166,029 people died from Covid-19 worldwide as of April

* Corresponding author at: Laboratoire de Biologie-Pathologie (Bat. I), Service des Agents Infectieux et d'Hygiène, Hôpital Nord, CHU de St-Etienne. Avenue Albert Raimond, 42270, St-Priest-en-Jarez, France.
E-mail address: paul.verhoeven@univ-st-etienne.fr (P.O. Verhoeven).
[1] These authors contributed equally.

https://doi.org/10.1016/j.jtemb.2021.126818
Received 13 December 2020; Received in revised form 8 June 2021; Accepted 6 July 2021
Available online 8 July 2021

30th, 2021 [4]. Thus, there is an urgent need to contain SARS-CoV-2 spread and virulence with effective curative and preventive treatments [2,3].

During the early phase of the SARS-CoV-2 outbreak, we have been faced with a strong need for *in vitro* models able to test the efficacy of compounds against this virus but only a few laboratories were able to do so. *In silico* studies have identified dozens of drugs potentially active against SARS-CoV-2 [5–10]. Drug repurposing is one of the most promising strategies for improving the care of Covid-19 patients but published data on the *in vitro* efficacy of molecules potentially active on SARS-CoV-2 remain very limited to date [11–14]. Available studies focused mostly on few drugs including hydroxychloroquine, remdesivir, lopinavir, ritonavir, interferon, umifenovir, favipiravir, camostat mesylate and immunomodulatory therapies [10,12–14].

Although some treatments have shown some benefits in patients at later stages of the disease (i.e. dexamethasone, anticoagulation treatments), there are no acknowledged effective antiviral therapies for Covid-19 [1]. Recently, preliminary results of the SOLIDARITY trial showed that hydroxychloroquine, remdesivir, lopinavir/ritonavir, and interferon regimens have no significant effect on the mortality rate nor on the length of hospital stay in COVID-19 patients [15]. Other ongoing clinical trials could provide additional results shortly [16].

Among the other compounds found to be directly active against SARS-CoV-2, essential minerals may require special attention. Antimicrobial and antiviral activity of copper is well established [17]. Copper ions have been found to elicit a broad action against viruses including coronaviruses [18–21]. Recently, it has been shown that SARS-CoV-2 can be eradicated from a copper surface within 4 h while it can survive up to 72 h on stainless steel and plastic surface [22]. Copper has been proposed to prevent transmission of the SARS-CoV-2 in the hospital environment (i.e. to cover door handles) or in application to face masks with the aim of reducing the risk of catching or spreading SARS-CoV-2 [21,23].

In eukaryotes, copper acts as an essential cofactor for more than 30 enzymes involved in redox reactions including superoxide dismutase (SOD) and ceruloplasmin. As well as for other trace metal ions (*e.g.* iron, manganese, zinc, selenium, and cobalt), maintenance of an adequate intracellular concentration of copper is essential to avoid the negative metabolic effects [24,25]. In humans, the normal cupremia varies from 9.75 to 27.75 μmol/L (650–1850 μg/L) in adults [24,26–28] and in tissues copper concentration range from 1 to 12 μg/g of tissues [24,28,29]. In human cells, copper is internalized by copper transporter 1 and is used for the synthesis of copper-requiring enzymes; it is stored mainly in the mitochondria and secreted by cells in the bloodstream; excess of copper is mostly eliminated by hepatocyte in bile [24]. In physiological conditions, copper is bound to ceruloplasmin (accounting for 40–70 % of total plasma copper), albumin, alpha-2 macroglobulin, and other copper-carrying proteins for avoiding uncontrolled redox activity [24,29].

To the best of our knowledge, no published study to date have evaluated the effect of copper gluconate using an *in vitro* cell model of SARS-CoV-2 infection. This study aimed to assess if pre- and post-exposure treatment with copper gluconate could prevent the cells to be infected. For this purpose, we developed an original confocal microscopy-based high content screening (HCS) method using a recombinant GFP expressing SARS-CoV-2.

2. Methods

2.1. Cells lines

Vero E6 cells (ATCC CRL-1586, ATCC) are kidney epithelial cells extracted from an African green monkey, which are widely used to study SARS-CoV-2 physiopathology. BHK-21 cells (CCL-10, ATCC) are kidney fibroblasts isolated form baby hamster and are useful for transformation and transfection purposes. These two cells lines were cultured in Dulbecco's modified Eagle's medium (DMEM, ref. D6429, Sigma-Aldrich, Saint Quentin Fallavier, France) supplemented with 2% foetal bovine serum (FBS) (ref. 10270106, Gibco, ThermoFisher, Courtaboeuf, France) without antibiotic. All cells were maintained at 37 °C and in a 5% CO_2 atmosphere.

2.2. Measurement of cell toxicity

To determine the toxicity of the chemical compound, cells were exposed to different concentrations of copper gluconate (Copper di-D-gluconate, CAS number 527-09-3, batch number 4891, 98.6 % purity, Isaltis, Lyon, France) ranging from 0 to 1600 μM for 24, 48 and 72 h in DMEM 2% FBS. Cell viability was determined in three independent experiments with the CyQUANT XTT assay (ref. × 12223, Invitrogen, ThermoFisher) following the manufacturer's recommendations. Optical densities at 450 nm (i.e. the XTT-specific absorbance) and at 660 nm (i.e the non-specific background signal contributed by cell and plastic-specific absorbance) were measured using a microplate reader (Sunrise, Tecan, Lyon, France). The toxicity of copper gluconate was also evaluated by propidium iodide assay with the same concentrations and incubation periods. Briefly, Vero E6 cells were labelled with 2 μg/mL of Hoechst 33342 (ref. H1399, Invitrogen) to count total number of cells, and with 2 μg/mL propidium iodide (ref. P3566, Invitrogen) to detect dead cells. Cells were imaged by confocal microscopy at 20-fold-magnification (Ti2 CSU-W1 SoRA, Nikon, France). Three independent experiments were performed and z-stack images were acquired in 12 random fields in duplicate wells (i.e. 6 fields per well) for each experimental condition. The whole process of acquisition was fully automated using in house pipeline developed with the JOBS module of the NIS software. Propidium iodide fluorescence was detected using a 561-nm laser for excitation and a 600/52 nm emission filter. Images were analyzed using NIS general analysis 3 in-house pipeline (NIS software v5.30, Nikon) to count the nuclei labeled in red and blue.

2.3. Production of GFP expressing SARS-CoV-2 particles

The bacterial artificial chromosome (BAC) containing viral cDNA of synSARS-CoV-2-GFP clone 6.2 was kindly provide by Volker Thiel [30]. Upon receipt, BAC was stored in *Saccharomyces cerevisiae* VL6-48 N strain [31], which was grown on YPD agar supplemented with 25 μg/mL of chloramphenicol. The yeast artificial chromosome (YAC) DNA was extracted using spin column-based nucleic acid purification (ZR BAC DNA Miniprep Kit, ref. D4049, Zymo Research, Irvine, CA). The YAC containing viral cDNA was transformed into *E. coli* TransforMax Epi300 (Ref. EC300110, Epicentre, Madison, WI) and amplified in LB broth supplemented with 25 μg/mL of chloramphenicol flowing manufacturer recommendations. The BAC was extracted from *E. coli* TransforMax Epi300 using spin column-based nucleic acid purification (ZR BAC DNA Miniprep Kit) and stored at 2−8 °C until used in the next days. The BAC containing viral cDNA was cleaved at a unique restriction site located downstream of the 3'-end poly(A) tail using NotI-HF (Ref. R3189S, NEB, Grenoble, France). In parallel, the gene coding for the nucleocapsid (N protein) was amplified from the BAC containing viral cDNA with a high fidelity polymerase (Taq Q5Hot Start High-Fidelity 2x Master Mix, Ref. M0494S, NEB) and primers PV012-F (5'-ACT-GTA-A-TA-CGA-CTC-ACT-ATA-GGG-ATG-TCT-GAT-AAT-GGA-CCC-CAA-AAT-C-3') and PV013-R (5'-GGC-CGC-GGC-CGC-TTT-TTT-TTT-TTT-TTT-TTT-TTT-TTT-TAG-GCC-TGA-GTT-GAG-TCA-GC-3'). *In vitro* transcription of 1−2 μg of phenol-chloroform extracted and ethanol precipitated DNA resolved in nuclease-free water was carried out using T7 RiboMAX expression large scale RNA production system (ref. P1300, Promega, Charbonnières-les-Bains, France) with m7G(5')ppp(5')G RNA Cap Structure Analog (ref. S1404L, Promega) as recommended by the manufacturer. A similar protocol was used to produce a capped mRNA encoding the N protein. Approximately 10 μg of *in vitro* transcribed viral genomic RNA was electroporated together with 2 μg of the N gene

transcript into BHK-21 cells. Briefly, 10^7 BHK-21 cells were resuspended in 350 μL of ice-cold PBS, mixed with RNA, and transferred to 0.2 cm electroporation cuvette. Electroporation was carried out with a Gene-pulser apparatus (ref. 1652660, Biorad, Marnes-La-Coquette, France) with one pulse of 140 V and 25 msec. BHK-21 electroporated cells were immediately co-cultivated with 70–80 % confluent Vero E6 cells in wells of 9.5 cm^2. After an incubation of cells for 5 days, the cell supernatant was collected and cellular residues were removed by centrifugation at 3000 *g* for 20 min. Clarified supernatant (passage 0) was stored and used to produce virus stocks for further analysis. All work involving the culture, production, and storage of SARS-CoV-2-GFP was performed in a biosafety level 3 (BSL3) laboratory.

2.4. Infection of Vero E6 cells with GFP expressing SARS-CoV-2

Copper gluconate was dissolved in sterile water and filter-sterilized with a 0.22 μm PVDF filter. The stock solution at 10 mM was stored at 2−8 °C for a maximum of 10 days. Vero E6 cells were seeded in a 96-well plate (ref. CLS3904, Corning, Sigma Aldrich) at a density of 20,000 cells per well. Cells were incubated for 18−24 h hours at 37 °C and in 5% CO_2. Then cells were incubated in cell medium with or without copper gluconate for 18−24 h hours. Next, the medium was removed before the cell being infected with GFP expressing SARS-CoV-2 at a multiplicity of infection (m.o.i) of 0.005 for 1 h. After the adsorption step, the medium was removed and cells were incubated at 37 °C and in 5% CO_2 for another 48 h-period in fresh medium (DMEM supplemented with 2% of FBS) supplemented with copper gluconate concentrations ranging from 0 to 100 μM with or without BSA (Ref. 1000-70, SEQENS *in vitro* diagnostic, France). Nuclei of Vero E6 cells were stained with 4 μg/mL Hoechst 33342 (ref. H1399, Invitrogen) for 30 min.

2.5. Confocal microscopy-based high content screening

Ninety-six-well plates were sealed in the BSL3 laboratory to be imaged by confocal microscopy at 40-fold-magnification (Ti2 CSU-W1 SoRA, Nikon, France). Three independent experiments were performed and z-stack images were acquired in 12 random fields in duplicate wells (i.e. 6 fields per well) for each experimental condition. The whole process of acquisition was fully automated using in house pipeline developed with the JOBS module of the NIS software. GFP fluorescence was detected using a 488-nm laser for excitation and a 525/50 nm emission filter. Hoechst fluorescence was detected using a 405-nm laser for excitation and a 447/60 nm emission filter. Images were analysed using NIS general analysis 3 in-house pipeline (NIS software v5.30, Nikon) to count the total number of nuclei, the number of nuclei in the infected area, the volume of the infected area, and the mean fluorescence intensity (MFI) of infected cells.

2.6. Statistics and software

SnapGene software v5.2 (GSL Biotech, San Diego, CA) was used to determine *in silico* the restriction profiles of BAC/YAC containing viral cDNA of synSARS-CoV-2-GFP clone 6.2. Statistical analysis and graphics were computed with GraphPad software v9.1 (Prism, San Diego, CA). The improvement of the images for publishing was performed with Fiji software (v1.53c).

3. Results

3.1. Cell toxicity of copper gluconate

Vero E6 cells were treated with gluconate copper concentrations ranging from 0 to 1600 μM for 24, 48 and 72 h. Cell viability was determined by measuring the reduction of XTT converted to orange-coloured formazan product using the CyQUANT XTT assay. The viability of Vero E6 treated with copper gluconate up to 200 μM was similar to that of untreated cells. However, the cell viability dropped below 70 % at 400 μM after 72 h and reached a value close to zero (or zero) for a concentration of 800 μM and 1600 μM after 48 h of treatment (Fig. 1a, b and c). Similar results were observed by measuring the percentage of dead cells with propidium iodide staining. Copper gluconate toxicity was found to increase over the time (Fig. 1d). At 72 h, no toxicity was observed up to 100 μM (Fig. 1d).

The cell viability was measured by XTT assay after an incubation-period of 24 h **(a)**, 48 h **(b)** and 72 h **(c)** in culture medium supplemented with copper gluconate. The ratio of viable cells was calculated by dividing the signal of treated cells by the signal of untreated cells multiplied by 100. Dots represent the value of each independent experiment, which correspond to the mean value of duplicate wells. Bars represent the mean value of three independent experiments. Error bars represent the standard deviation of the mean. The cell toxicity was measured by detecting cells that incorporate propidium iodide assay **(d)**. The percentage of dead Vero E6 cells was calculated by dividing the number of dead cells (nuclei labelled with propidium iodide) by the total number of cells (nuclei labelled with Hoechst). Dots represent the mean value of 36 microscopy fields at 20-fold-magnification (three independent experiments with duplicate wells, 6 fields per well). Colored areas around the connecting line represent the standard deviation of the mean.

3.2. Antiviral activity of copper gluconate treatment before viral infection

Vero E6 cells were treated with concentrations of copper gluconate ranging from 0 to 100 μM at 18−24 hours before SARS-CoV-2-GFP infection. The treatment was removed during the 1 h of the adsorption of recombinant SARS-CoV-2-GFP viruses. After adsorption, the medium was replaced by fresh culture media supplemented with the same concentrations of copper gluconate and cells were incubated for another 48 h-period to let viruses infect and replicate in cells. Then, the level of infection was measured by confocal microscopy. Results of three independent experiments are depicted in Fig. 2. The cumulative number of cells analysed in three independent experiments represents roughly 5000 cells per condition tested in each independent experiment. The rate of infection was significantly lower in cells treated with a concentration of copper gluconate of 25 μM and higher as compared to untreated cells (Fig. 2a). The rate of infection was 23.8 %, 18.9 %, 20.6 %, 6.9 %, 5.3 %,5.2 % in cells supplemented with 0, 2, 10, 25, 50 and 100 μM of copper gluconate respectively. Thus, the number of infected cells was reduced by 71, 77, and 78 % with 25, 50, and 100 μM of copper gluconate respectively ($p < 0.05$). The volume filled by infected cells was determined by measuring the volume filled by GFP-positive voxels. Again, the concentration of copper gluconate of 25 μM was the lowest dose tested that significantly reduced the viral infection as compared to untreated cells (Fig. 2b). Together, these results suggest that copper gluconate mitigate the infection of Vero E6 cells. Additionally, linear regression analysis showed that the MFI of infected cells decreased with the concentration of copper gluconate used to treat the cells ($p < 0.01$, linear regression) (Fig. 2c). These latter results suggest that copper gluconate might also limit the viral replication inside Vero E6 cells.

3.3. Antiviral activity of copper gluconate treatment after viral infection

To assess the effect of copper gluconate after the cells were infected, the same protocol was used except that Vero E6 cells were maintained in medium without copper gluconate until the infection step was performed. After adsorption, the medium was replaced by a fresh medium supplemented with concentrations of copper gluconate ranging from 0 to 100 μM and cells were incubated for an another 48 h-period. Results of three independent experiments are depicted in Fig. 2. The rate of infection was 28.1 %, 29.3 %, 25.6 %, 19.6 %, 15.2 %, 7.5 % in cells supplemented with 0, 2, 10, 25, 50 and 100 μM of copper gluconate respectively. The rate of infection decreased by 73 % in cells treated

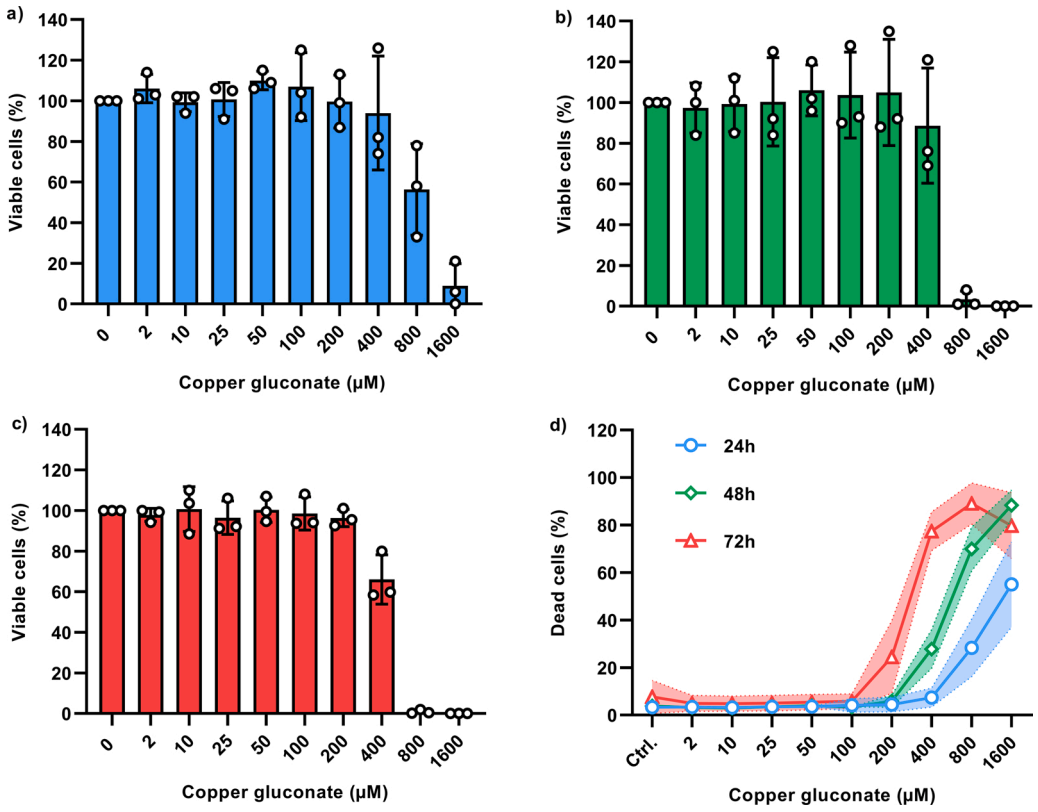

Fig. 1. Viability of Vero E6 incubated with copper gluconate.

with a concentration of copper gluconate of 100 μM as compared to untreated cells ($p < 0.05$) (Fig. 2d). In cells already infected, the 100 μM concentration of copper gluconate was the lowest dose tested that significantly reduced the viral infection as compared to untreated cells (Fig. 2e and f). In addition, we performed the same experiments with medium supplemented with 10–40 mg/l of BSA. Upon the addition of 10 mg/l of BSA to the medium, the antiviral effect of copper gluconate was abolished. With 10 mg/l of BSA, the infection rate was 29.9 %, 26.8 %, 34.0 % and 23.4 % in cells supplemented with 0, 25, 50 and 100 μM of copper gluconate respectively. Similar results were obtained with 20 mg/l and 40 mg/l of BSA (i.e. the absence of antiviral effect of copper gluconate). These results showed that albumin is able to completely inhibit the antiviral effect of the gluconate suggesting that the antiviral activity of copper gluconate observed *in vitro* will not be retained in serum where the albumin concentration is high.

4. Discussion

For this study, we developed an original confocal microscopy-based HCS using an *in vitro* model with Vero E6 cells challenged with a recombinant GFP expressing SARS-CoV-2 that was reconstructed using a yeast-based reverse genetics platform [30]. This method has the advantage of being able to analyse each cell individually and to count thousands of cells per well at the same time to increase the reliability of the observations. By using both a motorized stage and a fully automated pipeline for image recording, we virtually eliminated any possible bias that could be linked to the person in charge of image acquisition. The quantitative analysis of images was also fully automated by using an in-house pipeline developed with a plugin of the NIS software to avoid technical bias. A similar experimental setup with Vero E6 cells and the same GFP expressing SARS-CoV-2 clone was found to be suitable for drug screening applications by using the antiviral remdesivir as a reference [30]. Thus, we decided to combine this *in vitro* model of GFP expressing SARS-CoV-2 infection with confocal microscopy-based HCS to assess the antiviral activity of copper gluconate. Furthers improvements of this technology (e.g. using cell lines with fluorescence reporters) could help to study more easily whether and how drugs or chemical compounds could counteract SARS-CoV-2 infection in mammalian cells.

In the present study, we observed that the combination of pre- and post-exposure treatment of Vero E6 cells with copper gluconate at a concentration as low as 25 μM led to a 71 % reduction of the cell infection rate. When the cells were treated after the infection step, the concentration of copper gluconate needed for reducing by 70 % the infection rate was 100 μM. In any case, we could not observe a complete inhibition of the viral infection in this *in vitro* model. It must be acknowledged that the effect we observed with 25 μM of copper gluconate is not as powerful as that described with antiviral drugs [32]. In humans, the concentration of copper in whole blood is approximately 15 μM (1000 μg/L) [24,26–29]. Depending on the tissue, the copper concentration range from 1 to 12 μg/g, which is 1000-fold lower than the serum concentration [28,29]. It is important to note that almost all of the copper in the blood is tightly bound to components and not free to interact with cells, except to enter through specific transporters. In our *in vitro* model, the addition of albumin at physiological concentration (40 mg/L) and lower (20 mg/L and 10 mg/L) abolished the antiviral effect of copper gluconate suggesting that complexed copper no longer had an effect on the virus. Because of its high affinity for copper, albumin is known to be one of the main copper-binding components in mammalian blood plasma [29]. We observed that the addition of BSA inhibits antiviral activity of copper gluconate probably because free copper ions are bound by albumin and cannot be effective against SARS-CoV-2 viruses. *In vivo*, copper can also encounter various other proteins that can bind copper, and making it unavailable as an antimicrobial [29,44,45].

Even if copper seems to act against the virus by decreasing the number of infected cells, the mechanism of action is still far from being understood. The antiviral effect observed in Vero E6 cells with copper gluconate is probably multifactorial and certainly much more complex

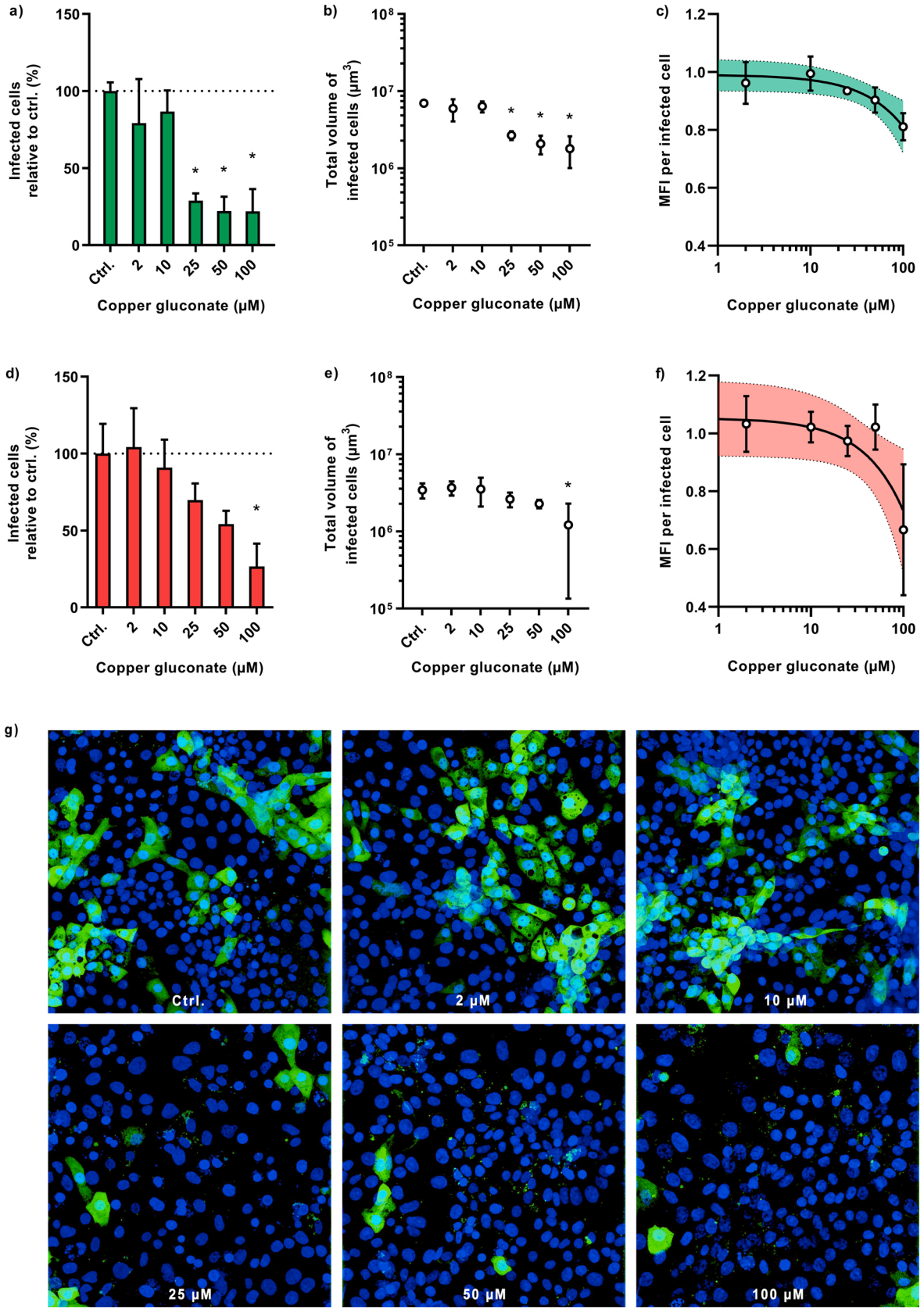

(caption on next page)

Fig. 2. Antiviral effect of copper gluconate on Vero E6 cells infected with GFP expressing SARS-CoV-2 at 48 h post-infection.
Vero E6 cells were incubated with **(a–c)** or without **(d–f)** copper gluconate for 18−24 h before SARS-CoV-2 infection. Cells were maintained with copper gluconate until 48 h post-infection. Confocal microscopy-based high content screening was used to measure the level of infection. Values represent the mean of three independent experiments and error bars represent the standard error of the mean. Rate of SARS-CoV-2 infected cells relative to control (untreated cells) **(a, c)**. Total volume filled by SARS-CoV-2 infected cells **(b, e)**. Mean fluorescence intensity (MFI) per infected cell. Solid line represents the linear regression ($p < 0.01$) with it 95 % confidence interval (filled area with doted lines) **(c, f)**. Vero E6 cells (nuclei in blue) infected with GFP expressing SARS-CoV-2 (GFP in green) with copper gluconate ranging from 0 (Ctrl.) to 100 μM (40-fold-magnification) **(g)**. Images represent the projection of image stacks using the extended deep focus (EDF) algorithm with the NIS software (v5.30). EDF images were merged, false-coloured, and contrast-enhanced with ImageJ software (v1.53c) for display purposes. * $p < 0.05$; values were compared by one-way ANOVA with Dunnet correction for multiple comparisons (for interpretation of the references to colour in this figure legend, the reader is referred to the web version of this article.).

in vivo. Warnes et al. showed that copper ions can damage virus membranes and destroy the viral genome of human coronavirus 229E [33]. In our study, a direct effect of copper cannot be excluded because copper gluconate was maintained in the culture medium as long as the infection lasted. We also observed that the increase of copper gluconate concentration up to 100 μM is associated with a statistically significant decrease of MFI. Because GFP expressed by the recombinant SARS-CoV-2 is fused to the non-structural protein 7, we can speculate that copper might limit the synthesis of viral proteins. This hypothesis is supported by *in silico* studies predicting that metal ions such as cobalt(III) or copper(II) could inhibit the SARS-CoV-2 main protease [34,35]. However, we found only two *in vitro* studies corroborating that copper ions could inhibit the synthesis of viral proteins or the replication cycle [36,37]. Thus, whether copper ions may limit the synthesis of viral proteins in mammalian cells is still far from being understood. *In vitro* studies showed that an increase of SOD1 expression is associated with a decrease in viral replication [38,39]. Further studies are needed to investigate whether the copper gluconate supplementation in culture media increases the internalization of copper and if intracellular copper is required to struggle against viral infection. Last, it was well established that the coronavirus replication complex requires autophagy-associated cellular components [40]. Because copper is known to be able to modulate autophagy, copper induced-autophagy could limit the availability of autophagy associated cellular components that are required for viral replication [19]. Whether one of these mechanisms more than another could be involved in the antiviral effect observed in our study remains unclear.

In vitro, we found that copper gluconate is well tolerate by Vero E6 cells even at strong concentration. It could be interesting to confirm these results with others cell lines but also with primary cells and human reconstructed epithelium. In our hand, we observed that very high concentrations over a limited period of 2 h could be used with no evidence of cytotoxicity after 24 h (Rigaill J, personal data). If the safety of local administration could be confirmed using *in vivo* models, it could be considered that copper gluconate delivered locally by mouthwashes or sprays could help to tackle the viruses produced by infected cells. By contrast, it is unlikely that copper keep an antiviral activity if administered by intravenous injection because copper is bound by albumin, ceruloplasmin and many other proteins [29,44,45]. The animal models of SARS-CoV-2 infection that have been developed worldwide [43] seems to be the most appropriate approach to assess the effect of copper administration during SARS-CoV-2 infection *in vivo*.

In humans, a retrospective observational study showed that zinc and selenium transporter selenoprotein P and zinc deficiency was associated with the worst outcomes in elderly Covid-19 patients [41]. A meta-analysis in Chinese children reported that copper deficiency is associated with recurrent respiratory tract infection [42]. Thus, it could be interesting to study copper concentrations in serum but also tissues such as nails and hairs in asymptomatic, mild, and severe Covid-19 patients.

In conclusion, our findings showed that copper gluconate is able to mitigate SARS-CoV-2 infection in Vero E6 cells but this effect was abolished by albumin, which suggests that copper will not retain its activity in serum. In the current context of active virus transmission, it is undoubtedly interesting to pursue the development of new therapeutic strategies in addition to vaccination efforts Furthers studies are still needed to investigate whether copper gluconate could be of benefit in mucosal administration such as mouthwash, nasal spray or aerosols

Author contributions

TB and POV designed the study. KR performed the rescue of recombinant SARS-CoV-2-GFP. FS, JR, EC, YD, AP performed experiments with infected cells. FS and AP performed cytotoxicity assays. POV and JR developed the pipeline and analysed the data. FS, TB, and POV wrote the manuscript. All authors reviewed the manuscript.

Funding

This research was funded by the University Jean Monnet of St-Etienne (emergency financing for a microscope), the University Hospital of St-Etienne (donation from the St-Etienne football club) and EA Pharma company. This latter company had no role in the study.

Roles in the study

TB and POV designed the study. KR performed the rescue of recombinant SARS-CoV-2-GFP. FS, JR, EC, YD, AP performed experiments with infected cells. FS and AP performed cytotoxicity assays. POV and JR developed the pipeline and analysed the data. FS, TB, and POV wrote the manuscript. All authors reviewed the manuscript.

Declaration of Competing Interest

The authors report no declarations of interest.

Acknowledgments

The BAC/YAC containing the viral cDNA of the recombinant GFP-expressing SARS-CoV2 was kindly provided by Prof. Volker Thiel (Bern University, Switzerland). The authors acknowledge Nadine Ebert and Fabien Labroussaa (Bern University, Switzerland) for their helpful advice for the rescue of the recombinant GFP-expressing SARS-CoV-2. The strain of *Saccharomyces cerevisiae* VL6-48N was generously provided by Carole Lartigue-Prat (Bordeaux University, France). The Vero E6 cell line (ATCC CRL-1586) was a gift of Prof. Bernard La Scola (Aix-Marseille University, France). Christophe Machu and Ibrahim Hassani from Nikon Company are acknowledged for their technical assistance and for the helpful discussion regarding the analysis of image stacks. Copper gluconate used for this study was provided free of charge by EA Pharma company.

References

[1] B. Hu, H. Guo, P. Zhou, Z.-L. Shi, Characteristics of SARS-CoV-2 and COVID-19, Nat. Rev. Microbiol. (2020), https://doi.org/10.1038/s41579-020-00459-7.
[2] D.L. McKee, A. Sternberg, U. Stange, S. Laufer, C. Naujokat, Candidate drugs against SARS-CoV-2 and COVID-19, Pharmacol. Res. 157 (2020) 104859, https://doi.org/10.1016/j.phrs.2020.104859.
[3] W.J. Wiersinga, A. Rhodes, A.C. Cheng, S.J. Peacock, H.C. Prescott, Pathophysiology, transmission, diagnosis, and treatment of coronavirus disease

2019 (COVID-19): a review, JAMA 324 (2020) 782–793, https://doi.org/10.1001/jama.2020.12839.
[4] COVID-19 Map, Johns Hopkins Coronavirus Resour. Cent. (n.d.), (accessed December 8, 2020), 2021, https://coronavirus.jhu.edu/map.html.
[5] A. Artese, V. Svicher, G. Costa, R. Salpini, V.C. Di Maio, M. Alkhatib, F. A. Ambrosio, M.M. Santoro, Y.G. Assaraf, S. Alcaro, F. Ceccherini-Silberstein, Current status of antivirals and druggable targets of SARS CoV-2 and other human pathogenic coronaviruses, Drug Resist. Updat. Rev. Comment. Antimicrob. Anticancer Chemother. 53 (2020), https://doi.org/10.1016/j.drup.2020.100721, 100721.
[6] R.R. Deshpande, A.P. Tiwari, N. Nyayanit, M. Modak, In silico molecular docking analysis for repurposing therapeutics against multiple proteins from SARS-CoV-2, Eur. J. Pharmacol. 886 (2020), https://doi.org/10.1016/j.ejphar.2020.173430, 173430.
[7] W.R. Ferraz, R.A. Gomes, A.L.S. Novaes, G.H. Goulart Trossini, Ligand and structure-based virtual screening applied to the SARS-CoV-2 main protease: an in silico repurposing study, Future Med. Chem. 12 (2020) 1815–1828, https://doi.org/10.4155/fmc-2020-0165.
[8] R. Pokhrel, P. Chapagain, J. Siltberg-Liberles, Potential RNA-dependent RNA polymerase inhibitors as prospective therapeutics against SARS-CoV-2, J. Med. Microbiol. 69 (2020) 864–873, https://doi.org/10.1099/jmm.0.001203.
[9] S. Sabarimurugan, A. Dharmarajan, S. Warrier, M. Subramanian, R. Swaminathan, Comprehensive review on the prevailing COVID-19 therapeutics and the potential of repurposing SARS-CoV-1 candidate drugs to target SARS-CoV-2 as a fast-track treatment and prevention option, Ann. Transl. Med. 8 (2020) 1247, https://doi.org/10.21037/atm-20-4071.
[10] D.E. Gordon, G.M. Jang, M. Bouhaddou, J. Xu, K. Obernier, K.M. White, M. J. O'Meara, V.V. Rezelj, J.Z. Guo, D.L. Swaney, T.A. Tummino, R. Hüttenhain, R. M. Kaake, A.L. Richards, B. Tutuncuoglu, H. Foussard, J. Batra, K. Haas, M. Modak, M. Kim, P. Haas, B.J. Polacco, H. Braberg, J.M. Fabius, M. Eckhardt, M. Soucheray, M.J. Bennett, M. Cakir, M.J. McGregor, Q. Li, B. Meyer, F. Roesch, T. Vallet, A. Mac Kain, L. Miorin, E. Moreno, Z.Z.C. Naing, Y. Zhou, S. Peng, Y. Shi, Z. Zhang, W. Shen, I.T. Kirby, J.E. Melnyk, J.S. Chorba, K. Lou, S.A. Dai, I. Barrio-Hernandez, D. Memon, C. Hernandez-Armenta, J. Lyu, C.J.P. Mathy, T. Perica, K.B. Pilla, S. J. Ganesan, D.J. Saltzberg, R. Rakesh, X. Liu, S.B. Rosenthal, L. Calviello, S. Venkataramanan, J. Liboy-Lugo, Y. Lin, X.-P. Huang, Y. Liu, S.A. Wankowicz, M. Bohn, M. Safari, F.S. Ugur, C. Koh, N.S. Savar, Q.D. Tran, D. Shengjuler, S. J. Fletcher, M.C. O'Neal, Y. Cai, J.C.J. Chang, D.J. Broadhurst, S. Klippsten, P. P. Sharp, N.A. Wenzell, D. Kuzuoglu-Ozturk, H.-Y. Wang, R. Trenker, J.M. Young, D.A. Cavero, J. Hiatt, T.L. Roth, U. Rathore, A. Subramanian, J. Noack, M. Hubert, R.M. Stroud, A.D. Frankel, O.S. Rosenberg, K.A. Verba, D.A. Agard, M. Ott, M. Emerman, N. Jura, M. von Zastrow, E. Verdin, A. Ashworth, O. Schwartz, C. d'Enfert, S. Mukherjee, M. Jacobson, H.S. Malik, D.G. Fujimori, T. Ideker, C. S. Craik, S.N. Floor, J.S. Fraser, J.D. Gross, A. Sali, B.L. Roth, D. Ruggero, J. Taunton, T. Kortemme, P. Beltrao, M. Vignuzzi, A. García-Sastre, K.M. Shokat, B. K. Shoichet, N.J. Krogan, A SARS-CoV-2 protein interaction map reveals targets for drug repurposing, Nature 583 (2020) 459–468, https://doi.org/10.1038/s41586-020-2286-9.
[11] I.A. Anastasiou, I. Eleftheriadou, A. Tentolouris, D. Tsilingiris, N. Tentolouris, In vitro data of current therapies for SARS-CoV-2, Curr. Med. Chem. 27 (2020) 4542–4548, https://doi.org/10.2174/0929867327666200513075430.
[12] A. Artese, V. Svicher, G. Costa, R. Salpini, V.C. Di Maio, M. Alkhatib, F. A. Ambrosio, M.M. Santoro, Y.G. Assaraf, S. Alcaro, F. Ceccherini-Silberstein, Current status of antivirals and druggable targets of SARS CoV-2 and other human pathogenic coronaviruses, Drug Resist. Updat. Rev. Comment. Antimicrob. Anticancer Chemother. 53 (2020), https://doi.org/10.1016/j.drup.2020.100721, 100721.
[13] J. Santos, S. Brierley, M.J. Gandhi, M.A. Cohen, P.C. Moschella, A.B.L. Declan, Repurposing therapeutics for potential treatment of SARS-CoV-2: a review, Viruses 12 (2020), https://doi.org/10.3390/v12070705.
[14] A. Simonis, S.J. Theobald, G. Fätkenheuer, J. Rybniker, J.J. Malin, A comparative analysis of remdesivir and other repurposed antivirals against SARS-CoV-2, EMBO Mol. Med. (2020) e13105, https://doi.org/10.15252/emmm.202013105.
[15] WHO Solidarity Trial Consortium, H. Pan, R. Peto, A.-M. Henao-Restrepo, M.-P. Preziosi, V. Sathiyamoorthy, Q. Abdool Karim, M.M. Alejandria, C. Hernández García, M.-P. Kieny, R. Malekzadeh, S. Murthy, K.S. Reddy, M. Roses Periago, P. Abi Hanna, F. Ader, A.M. Al-Bader, A. Alhasawi, E. Allum, A. Alotaibi, C. A. Alvarez-Moreno, S. Appadoo, A. Asiri, P. Aukrust, A. Barratt-Due, S. Bellani, M. Branca, H.B.C. Cappel-Porter, N. Cerrato, T.S. Chow, N. Como, J. Eustace, P. J. García, S. Godbole, E. Gotuzzo, L. Griskevicius, R. Hamra, M. Hassan, M. Hassany, D. Hutton, I. Irmansyah, L. Jancoriene, J. Kirwan, S. Kumar, P. Lennon, G. Lopardo, P. Lydon, N. Magrini, T. Maguire, S. Manevska, O. Manuel, S. McGinty, M.T. Medina, M.L. Mesa Rubio, M.C. Miranda-Montoya, J. Nel, E. P. Nunes, M. Perola, A. Portolés, M.R. Rasmin, A. Raza, H. Rees, P.P.S. Reges, C. A. Rogers, K. Salami, M.I. Salvadori, N. Sinani, J.A.C. Sterne, M. Stevanovikj, E. Tacconelli, K.A.O. Tikkinen, S. Trelle, H. Zaid, J.-A. Røttingen, S. Swaminathan, Repurposed antiviral drugs for Covid-19 - interim WHO solidarity trial results, N. Engl. J. Med. (2020), https://doi.org/10.1056/NEJMoa2023184.
[16] COVID-19 Studies From the World Health Organization Database - ClinicalTrials. gOv, 2021 (accessed December 8, 2020), (n.d.), https://clinicaltrials.gov/ct2/who_table.
[17] M. Vincent, R.E. Duval, P. Hartemann, M. Engels-Deutsch, Contact killing and antimicrobial properties of copper, J. Appl. Microbiol. 124 (2018) 1032–1046, https://doi.org/10.1111/jam.13681.
[18] A. Monette, A.J. Mouland, Zinc and copper ions differentially regulate prion-like phase separation dynamics of pan-virus nucleocapsid biomolecular condensates, Viruses 12 (2020), https://doi.org/10.3390/v12101179.
[19] A. Andreou, S. Trantza, D. Filippou, N. Sipsas, S. Tsiodras, COVID-19: the potential role of copper and N-acetylcysteine (NAC) in a combination of candidate antiviral treatments against SARS-CoV-2, Vivo Athens Greece 34 (2020) 1567–1588, https://doi.org/10.21873/invivo.11946.
[20] S. Raha, R. Mallick, S. Basak, A.K. Duttaroy, Is copper beneficial for COVID-19 patients? Med. Hypotheses 142 (2020) https://doi.org/10.1016/j.mehy.2020.109814, 109814.
[21] A.A. Cortes, J.M. Zuñiga, The use of copper to help prevent transmission of SARS-coronavirus and influenza viruses. A general review, Diagn. Microbiol. Infect. Dis. 98 (2020), https://doi.org/10.1016/j.diagmicrobio.2020.115176, 115176.
[22] N. van Doremalen, T. Bushmaker, D.H. Morris, M.G. Holbrook, A. Gamble, B. N. Williamson, A. Tamin, J.L. Harcourt, N.J. Thornburg, S.I. Gerber, J.O. Lloyd-Smith, E. de Wit, V.J. Munster, Aerosol and surface stability of SARS-CoV-2 as compared with SARS-CoV-1, N. Engl. J. Med. 382 (2020) 1564–1567, https://doi.org/10.1056/NEJMc2004973.
[23] D. Bradley, Copper against covid, Mater. Today Kidlington Engl. 40 (2020) 2–3, https://doi.org/10.1016/j.mattod.2020.09.016.
[24] P. Lelièvre, L. Sancey, J.-L. Coll, A. Deniaud, B. Busser, The multifaceted roles of copper in Cancer: a trace metal element with dysregulated metabolism, but also a target or a bullet for therapy, Cancers 12 (2020), https://doi.org/10.3390/cancers12123594.
[25] G. Weiss, P.L. Carver, Role of divalent metals in infectious disease susceptibility and outcome, Clin. Microbiol. Infect. 24 (2018) 16–23, https://doi.org/10.1016/j.cmi.2017.01.018.
[26] F. Pizarro, M. Olivares, R. Uauy, P. Contreras, A. Rebelo, V. Gidi, Acute gastrointestinal effects of graded levels of copper in drinking water, Environ. Health Perspect. 107 (1999) 117–121, https://doi.org/10.1289/ehp.99107117.
[27] F. Pizarro, M. Olivares, M. Araya, V. Gidi, R. Uauy, Gastrointestinal effects associated with soluble and insoluble copper in drinking water, Environ. Health Perspect. 109 (2001) 949–952, https://doi.org/10.1289/ehp.01109949.
[28] Agency for Toxic Substances and Disease Registry (ATSDR), Toxicological Profile for Copper, U.S. Department of Health and Human Services, Public Health Service, Atlanta, GA, 2004. https://www.atsdr.cdc.gov/toxprofiles/TP.asp?id=206&tid=37.
[29] M.C. Linder, Ceruloplasmin and other copper binding components of blood plasma and their functions: an update, Met. Integr. Biometal Sci. 8 (2016) 887–905, https://doi.org/10.1039/c6mt00103c.
[30] T.T.N. Thao, F. Labroussaa, N. Ebert, P. V'kovski, H. Stalder, J. Portmann, J. Kelly, S. Steiner, M. Holwerda, A. Kratzel, M. Gultom, K. Schmied, L. Laloli, L. Hüsser, M. Wider, S. Pfaender, D. Hirt, V. Cippà, S. Crespo-Pomar, S. Schröder, D. Muth, D. Niemeyer, V. Corman, M.A. Müller, C. Drosten, R. Dijkman, J. Jores, V. Thiel, Rapid reconstruction of SARS-CoV-2 using a synthetic genomics platform, Nature (2020), https://doi.org/10.1038/s41586-020-2294-9.
[31] N. Kouprina, V.N. Noskov, V. Larionov, Selective isolation of large segments from individual microbial genomes and environmental DNA samples using transformation-associated recombination cloning in yeast, Nat. Protoc. 15 (2020) 734–749, https://doi.org/10.1038/s41596-019-0280-1.
[32] M. Wang, R. Cao, L. Zhang, X. Yang, J. Liu, M. Xu, Z. Shi, Z. Hu, W. Zhong, G. Xiao, Remdesivir and chloroquine effectively inhibit the recently emerged novel coronavirus (2019-nCoV) in vitro, Cell Res. 30 (2020) 269–271, https://doi.org/10.1038/s41422-020-0282-0.
[33] S.L. Warnes, Z.R. Little, C.W. Keevil, Human coronavirus 229E remains infectious on common touch surface materials, MBio 6 (2015) e01697–01615, https://doi.org/10.1128/mBio.01697-15.
[34] R.A. Garza-Lopez, J.J. Kozak, H.B. Gray, Copper(II) inhibition of the SARS-CoV-2 main protease, ChemRxiv Prepr. Serv. Chem. (2020), https://doi.org/10.26434/chemrxiv.12673436.
[35] J.J. Kozak, H.B. Gray, R.A. Garza-López, Structural stability of the SARS-CoV-2 main protease: can metal ions affect function? J. Inorg. Biochem. 211 (2020) https://doi.org/10.1016/j.jinorgbio.2020.111179, 111179.
[36] J.L. Sagripanti, M.M. Lightfoote, Cupric and ferric ions inactivate HIV, AIDS Res. Hum. Retroviruses 12 (1996) 333–337, https://doi.org/10.1089/aid.1996.12.333.
[37] T.H. Sucipto, S. Churrotin, H. Setyawati, F. Martak, K.C. Mulyatno, I.H. Amarullah, T. Kotaki, M. Kameoka, S. Yotopranoto, A.S. Soegijanto, A new copper(II)-imidazole derivative effectively inhibits replication of DENV-2 in vero cell, Afr. J. Infect. Dis. 12 (2018) 116–119, https://doi.org/10.2101/Ajid.12v1S.17.
[38] A.M. Rivas-Estilla, O.L. Bryan-Marrugo, K. Trujillo-Murillo, D. Pérez-Ibave, C. Charles-Niño, C. Pedroza-Roldan, C. Ríos-Ibarra, E. Ramírez-Valles, R. Ortiz-López, M.C. Islas-Carbajal, N. Nieto, A.R. Rincón-Sánchez, Cu/Zn superoxide dismutase (SOD1) induction is implicated in the antioxidative and antiviral activity of acetylsalicylic acid in HCV-expressing cells, Am. J. Physiol. Gastrointest. Liver Physiol. 302 (2012) G1264–1273, https://doi.org/10.1152/ajpgi.00237.2011.
[39] X. Lin, R. Wang, W. Zou, X. Sun, X. Liu, L. Zhao, S. Wang, M. Jin, The influenza virus H5N1 infection can induce ROS production for viral replication and host cell death in A549 cells modulated by human Cu/Zn superoxide dismutase (SOD1) overexpression, Viruses 8 (2016), https://doi.org/10.3390/v8010013.
[40] E. Prentice, W.G. Jerome, T. Yoshimori, N. Mizushima, M.R. Denison, Coronavirus replication complex formation utilizes components of cellular autophagy, J. Biol. Chem. 279 (2004) 10136–10141, https://doi.org/10.1074/jbc.M306124200.
[41] R.A. Heller, Q. Sun, J. Hackler, J. Seelig, L. Seibert, A. Cherkezov, W.B. Minich, P. Seemann, J. Diegmann, M. Pilz, M. Bachmann, A. Ranjbar, A. Moghaddam, L. Schomburg, Prediction of survival odds in COVID-19 by zinc, age and

selenoprotein P as composite biomarker, Redox Biol. 38 (2020), https://doi.org/10.1016/j.redox.2020.101764, 101764.

[42] S. Mao, A. Zhang, S. Huang, Meta-analysis of Zn, Cu and Fe in the hair of Chinese children with recurrent respiratory tract infection, Scand. J. Clin. Lab. Invest. 74 (2014) 561–567, https://doi.org/10.3109/00365513.2014.921323.

[43] C. Muñoz-Fontela, W.E. Dowling, S.G.P. Funnell, P.-S. Gsell, A.X. Riveros-Balta, R. A. Albrecht, H. Andersen, R.S. Baric, M.W. Carroll, M. Cavaleri, C. Qin, I. Crozier, K. Dallmeier, L. de Waal, E. de Wit, L. Delang, E. Dohm, W.P. Duprex, D. Falzarano, C.L. Finch, M.B. Frieman, B.S. Graham, L.E. Gralinski, K. Guilfoyle, B.L. Haagmans, G.A. Hamilton, A.L. Hartman, S. Herfst, S.J.F. Kaptein, W.B. Klimstra, I. Knezevic, P.R. Krause, J.H. Kuhn, R. Le Grand, M.G. Lewis, W.-C. Liu, P. Maisonnasse, A. K. McElroy, V. Munster, N. Oreshkova, A.L. Rasmussen, J. Rocha-Pereira, B. Rockx, E. Rodríguez, T.F. Rogers, F.J. Salguero, M. Schotsaert, K.J. Stittelaar, H.J. Thibaut, C.-T. Tseng, J. Vergara-Alert, M. Beer, T. Brasel, J.F.W. Chan, A. García-Sastre, J. Neyts, S. Perlman, D.S. Reed, J.A. Richt, C.J. Roy, J. Segalés, S.S. Vasan, A. M. Henao-Restrepo, D.H. Barouch, Animal models for COVID-19, Nature. 586 (2020) 509–515, https://doi.org/10.1038/s41586-020-2787-6.

[44] G. Borkow, J. Gabbay, Copper, An Ancient Remedy Returning to Fight Microbial, Fungal and Viral Infections, Curr. Chem. Biol. 3 (2009) 272–278, https://doi.org/10.2174/187231309789054887.

[45] I. Scheiber, R. Dringen, J.F.B. Mercer, Copper: effects of deficiency and overload, Met. Ions Life Sci. 13 (2013) 359–387, https://doi.org/10.1007/978-94-007-7500-8_11.